Bollettino di Geofisica Teorica ed Applicata Vol. 58, n. 4, pp. 265-284; December 2017
DOI 10.4430/bgta0195

Stress and strain-rate fields: a comparative analysis for the Italian territory

B. Mastrolembo and A. Caporali

Dipartimento di Geoscienze, Università di Padova, Italy

(Received: February 21, 2017; accepted: June 8, 2017)

ABSTRACT We present a comparative analysis between the contemporary Italian crustal stress map and the strain-rate field inferred from GPS velocities. We use the most complete and updated stress map of Italy which consists of 630 data mainly from borehole breakouts, earthquake focal mechanisms, and active faults with an unprecedented spatial coverage of several tectonic areas within the Italian territory. Stress and strain rate are physical quantities, linked by a causal relationship, with parallel eigenvectors in case of a perfectly elastic mean. Comparing surface geodetically inferred strainrate orientations with the stress measured in the crust allows a quantitative analysis of the relation between surface deformation and deep tectonic processes acting at the different depths in the brittle crust. Data from over 500 GPS stations with a minimum time span of 2 years are weekly analyzed, according to the international standards, to estimate a velocity field aligned with the ITRF frame (IGb08). We use a least-squares collocation algorithm to interpolate the horizontal GPS velocities and estimate the strain-rate eigenvectors at the position of those stress data surrounded by a sufficient number of GPS stations. The stress data set consists of borehole breakout (305, A-D quality) and earthquake focal solution (392, C quality) measurements. We identify five tectonic provinces covered by a large population of GPS sites and rather homogeneous stress orientations: three of them, Friuli, Emilia, and outer Apennines area undergoing compression, while central and southern Apennines are subject to extension perpendicular to the belt axis. We compute the difference in azimuth of minimum horizontal stresses between each breakout or focal mechanism measurement, and the geodetically inferred direction. Our analysis shows that the geophysical and geodetic measurements predict in most cases (~60%) the same orientation for the crustal stress and surface strain-rate tensors, within one standard deviation. The largest azimuthal differences (>80°) are observed in the outer Apennines area for a few stress data from focal solutions of relatively deep events. This might suggest that the observed strainrate at the Earth surface is decoupled from deformation processes at crustal depth.

Key words: contemporary stress data, strainrate, Global Positioning System, tectonics.

1. Introduction

The knowledge of the contemporary state of stress in the Earth crust comes from a variety of sources and techniques such as earthquake focal mechanisms, fault data, borehole breakouts

in deep wells and seismic sequence data. In-situ measurements are confined to a depth of few km, whereas focal mechanisms represent a stress indicator up to the lower boundary of the seismogenic layer, typically ~20 km. Results from the World Stress Map Project (WSM; http://www.world-stress-map.org; Zoback, 1992; Heidbach *et al.,* 2016) have shown that stress orientations throughout the brittle upper crust are quite homogeneous and representative of the regional tectonic stress. In the most recent works relying on a large number of stress data (Heidbach *et al.,* 2010; Yang and Hauksson 2013; Montone and Mariucci, 2016), the multi-wavelength nature of the stress field is described as a three-orders pattern where broad areas of uniform crustal stress (wavelength >500 km) are interspersed by regional (100-500 km) to local (<100 km) heterogeneities typically related to active faulting, topography, gravitational collapse or density contrasts.

The updated present-day Italian Stress Map (Fig. 1), published (2016), by Montone and Mariucci, contains 630 data mostly from the analysis of borehole breakouts, focal mechanisms and active faults. This unprecedented database allows to identify third-order patterns of the Italian stress field that, as argued by Pierdominici and Heidbach (2012), has a predominant wavelength of ~150 km. Stress directions estimated by Montone and Mariucci (2016) are consistent with the previous maximum horizontal compressive stress azimuths statistically interpolated by Carafa and Barba (2013) on the base of the WSM 2008 data set (Heidbach *et al.,* 2008).

On the other hand, the measurement of the horizontal gradient of GPS velocities is related to the present day strain rate at the Earth surface. Classically, strain-rate eigenvectors are estimated through the interpolation of velocities from at least three GPS sites (e.g., Haines and Holt, 1993; Shen *et al.,* 1996; Caporali *et al.,* 2003; Kréemer *et al.,* 2014). Geophysical data provide the direction of the principal stresses of a very localized area, whereas geodetic data entail average strain-rate values representative of areas of a few tens of kilometres. For dense GPS networks in regions subjected to active deformation of a wavelength larger than the spacing between the GPS sites, the average strain rate and stress directions should be comparable, provided that the geodetically inferred deformation on the surface remains constant at the average depth of the stress measurements. The principal directions of the strain-rate tensor coincide with those of the stress rate, in a plane stress approximation, assuming that stress and strain are linearly dependent, i.e., an elastic rheology. This assumption is acceptable if we confine to the brittle upper crust.

Palano (2015) carried out an analysis of stress and strain-rate fields of Italy. He performed a comparison of GPS inferred strain-rate data and 308 stress data interpolated at each node of a regular grid. Here, we present a direct comparison of principal horizontal directions of stress and strain-rate directions of extension estimated, using a collocation algorithm (Caporali *et al.,* 2003), at the position of each stress measurement in our data set. We use GPS data coming from over 500 stations distributed on the Italian peninsula (Fig. 2) and weekly processed at the University of Padova using EUREF processing standards (Bruyninx *et al.,* 2013). Wherever the distribution of the GPS sites provides a redundant coverage of the area of interest, the geodetic strain-rate tensor is interpolated at the location of wells and focal mechanism solutions in the Italian stress map. We use all the stress orientations from earthquake focal mechanisms (392 data with maximum uncertainty of 25°) whereas we select only A-D quality stress data from borehole breakouts (305 data, uncertainty <40 degrees; Fig. 1). We define five provinces (Friuli, Emilia, and central, outer and southern Apennines; polygons in Fig. 1) characterized by rather

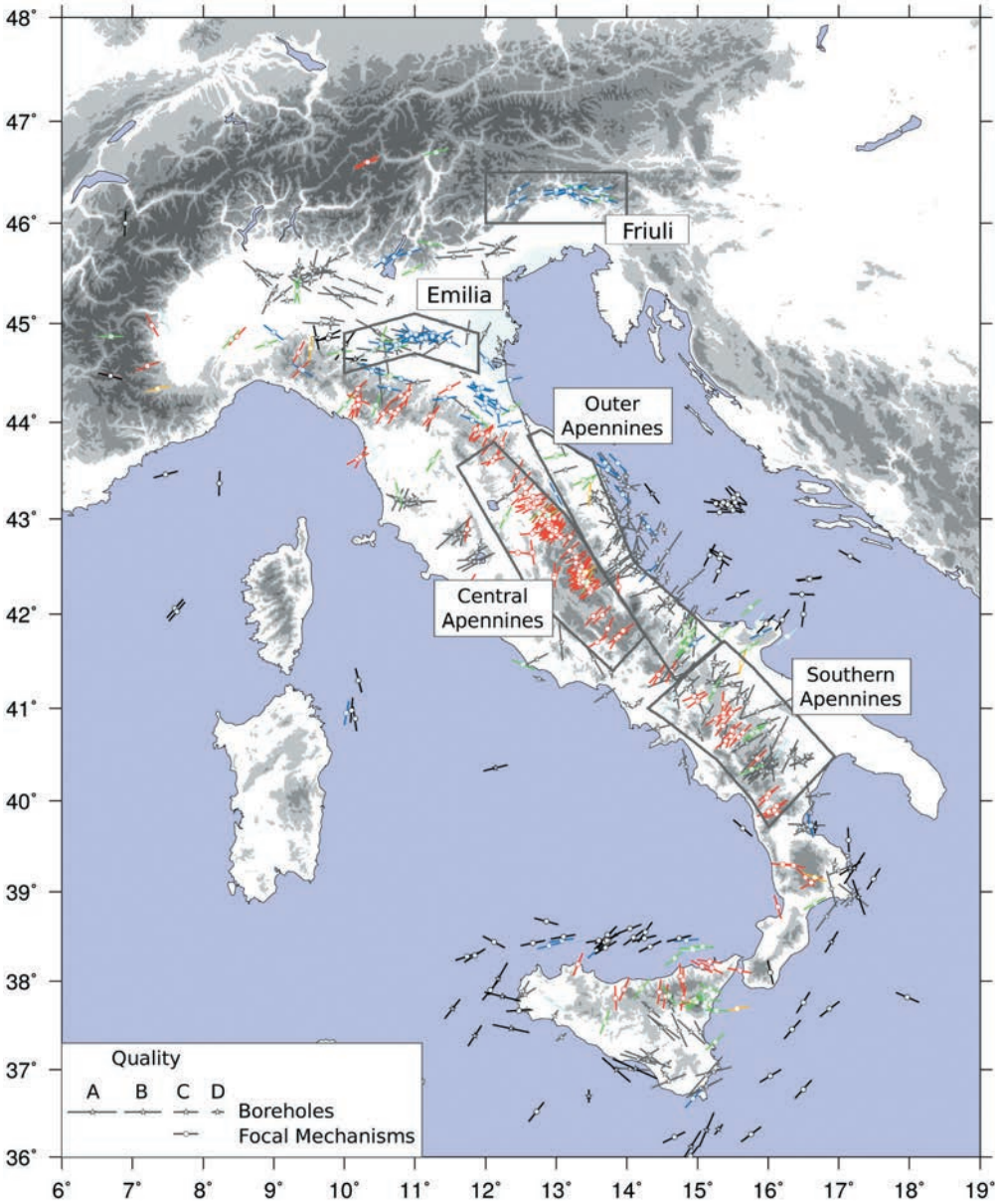

Fig. 1 - Minimum horizontal stress orientations from Montone and Mariucci (2016). Only data from borehole (dash with star) and focal mechanisms (dash with circle) are used in this work. Quality ranks (A-D) are represented as a four level length scale of the dashes. As in Montone and Mariucci (2016), colors represent the tectonic regime (red: normal-faulting, yellow: normal-strike, green: strike-slip, blue: thrust, light blue: thrust-strike). Black symbols refer to stress data for which the geodetic strainrate is not estimated. Grey polygons represent the five analyzed tectonic regions (Friuli, Emilia, central Appenines, outer Apennines and southern Apennines).

homogeneous tectonic regimes and well covered by GPS sites as well as by stress data and calculate the angular differences between geodetic and geophysical minimum horizontal stress orientations. We show that, overall, the two data sets agree within given tolerance for all the study areas. The residuals have a nearly random distribution around zero with a rms (root mean square) spread comparable with the uncertainty of the stress data.

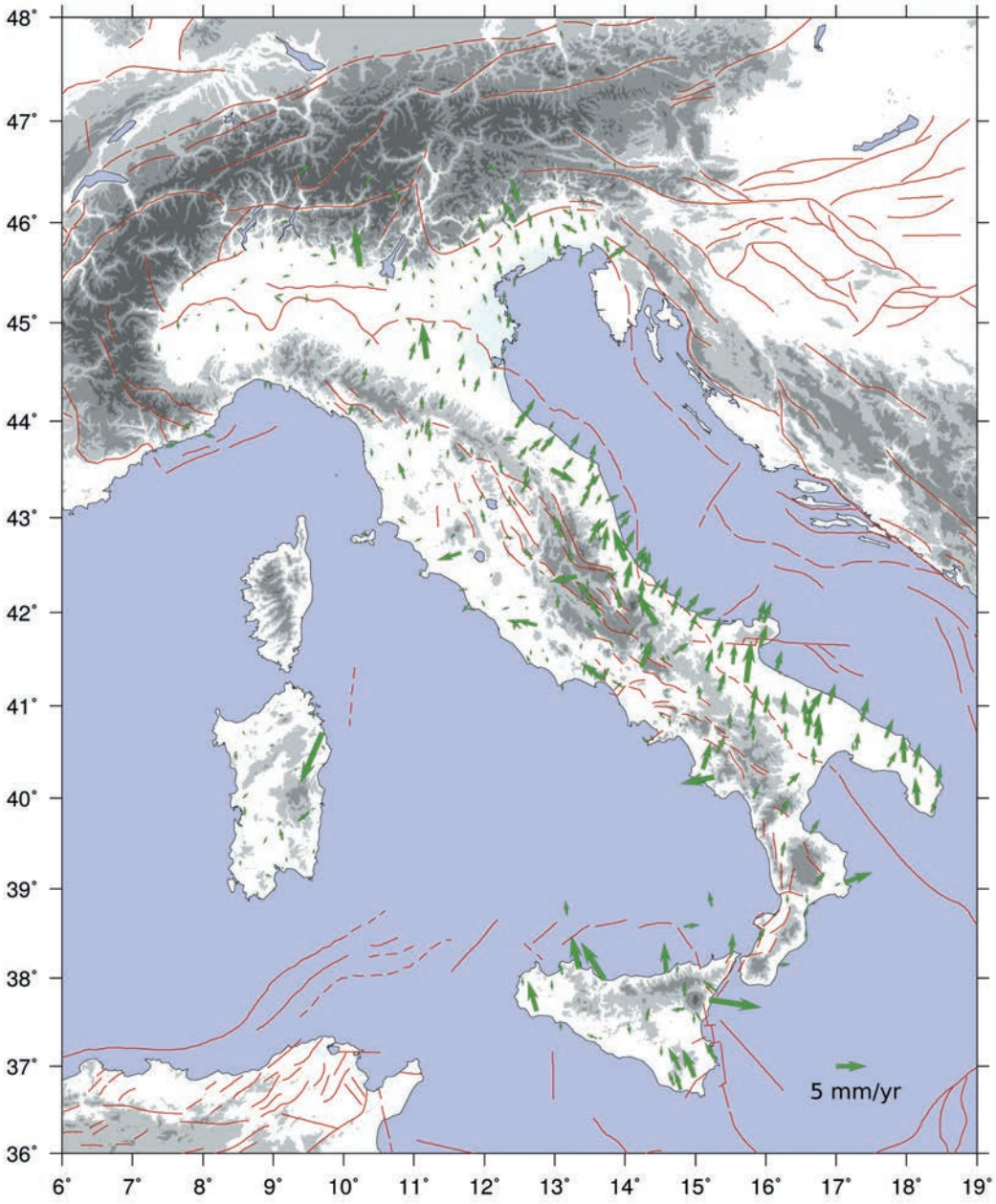

Fig. 2 - Horizontal GPS velocities given with respect to the Eurasian Plate from continuous stations processed at the University of Padova. Red lines show major faults.

2. Crustal deformation of the Italian territory

Central Mediterranean represents a complex mosaic of plate and microplates whose kinematics is driven by the convergence of the almost rigid African and Eurasian Plates that, according to DeMets *et al*. (2010), takes place at a rate of ~7 mm/yr in NW-SE direction. At a smaller scale various geodynamic processes such as subduction, rifting, backarc spreading and faulting are observed in close proximity, leading to a strong variability of tectonic regimes.

Extensional, compressive and strike-slip structures coexist within short distances, producing different stress regimes and orientations.

GPS data together with seismicity distribution, geological and geophysical observations, represent a strong constraint to the identification of the main areas of deformation (e.g., Nocquet, 2012; Faccenna *et al.,* 2014).

Despite convergence is the overall process that controls the kinematics of the central Mediterranan region, the present-day active tectonics of Italy (Fig. 3) is dominated by the extension from the northern to the central and southern Apennines and compression along the Sicilian Maghrebides (e.g., Sgroi *et al.,* 2012; Sani *et al.,* 2016). Shortening is observed across the Po Plain, Montello, Friuli, and southern Tyrrhenian regions (e.g., Billi *et al*., 2011; Carafa and Bird, 2016; Serpelloni *et al.,* 2016). Strike slip regime is limited to the Gargano area where the Mattinata Fault displays an almost E-W right-lateral movement (Di Bucci *et al.,* 2009) and to north-eastern Sicily where a right-lateral strike slip lineament, running from the Aeolian to Malta island, separates the southern Tyrrhenian into two different seismotectonic areas (e.g., Serpelloni *et al*., 2005, 2010; Billi *et al.,* 2011; Mastrolembo *et al*., 2014). Strike slip active deformation is finally visible along the Giudicarie and Dinarides belts in the southern eastern Alps, as a consequence of the northward indentation of the Adria block (Kastelic and Carafa, 2012; Caporali *et al.,* 2013). The main seismogenic areas of the Italian territory are well depicted by the Database of Individual Seismogenic Sources (DISS: DISS Working Group, 2015). The repository includes, in addition to the Individual Seismogenic Sources (ISS), also the Composite Seismogenic Sources (CSS). These are elongated regions containing an unspecified number of aligned seismogenic ruptures that cannot be singled out but are characterized by high rates of seismicity (Fig. 3).

Apennines are a ~500 km long fold-and-thrust belt that runs in NW-SE direction and host most of the fastest slipping active normal faults (Valensise and Pantosti, 2001) and strongest seismic events of the Italian territory. Their tectonic evolution has been explained as driven by the retreating subduction of the Adriatic-Ionian lithosphere (Malinverno and Ryan, 1986; Faccenna *et al.,* 2001). Focal mechanisms data (Pondrelli *et al*., 2011; Fig. 3) along with in situ measurements (Montone and Mariucci, 2016; Fig. 1) display a predominance of extensional regime along the central Apennines with the main extensional axes perpendicular to the belt, while in the northern sector (Po Plain area) extension and shortening coexist in close proximity (e.g., Viti *et al*., 2015). In the Po Plain, thrust events usually show hypocentral depths greater than 20 km (Pondrelli *et al.,* 2006) suggesting a strict correlation with the passive sinking of the Adriatic lithosphere beneath the Apennine chain. Seismic tomographic data suggest slab detachment for the central Apennines (Wortel and Spakman, 2000), where various mechanisms have been discussed as source of the observed extensional faulting. Based on modelling of GPS data, D'Agostino *et al*. (2008) explained the extensional regime of Apennine belt as related to the NE-ward motion of Adria Plate relative to Eurasia. The nature of the forces controlling the extension in the Apennines is debated. D'Agostino *et al*. (2014) concluded that no subduction forces are needed to explain the active deformation within the Apennines, resulting from lateral variations in the gravitational potential energy of the lithosphere. On the other hand Carafa *et al*. (2015) point out that lithostatic pressure forces related to the gravitational potential energy do not suffice to generate extension along the Apennines, and external forces to the lithosphere are necessary (Barba *et al.,* 2008; Petricca *et al.,* 2013).

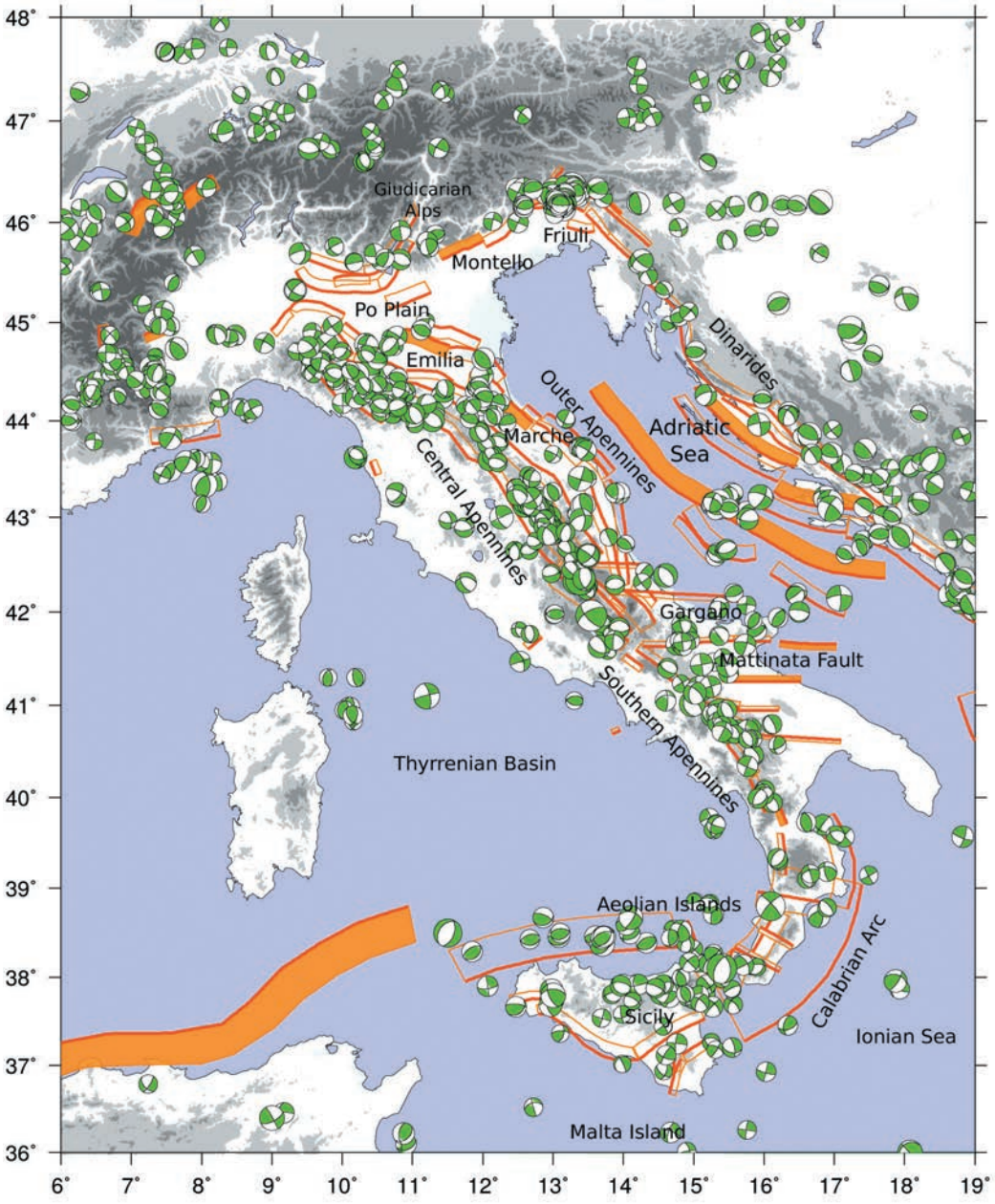

Fig. 3 - Seismotectonic map for central Mediterranean region. Earthquake focal mechanisms are taken from Harvard-CMT, INGV-RCMT, ETH-RMT and EMMA catalogues. Historical events between 1905 and 2010 with $M_w \geq 4$ are shown. Orange boxes represent the horizontal projection of the CSSs included in the DISS database, the dark orange line indicate fault traces. Main tectonic areas described in the text are indicated.

The active tectonics of outer northern Apennines is characterized in the outer belt by compression, with the orientation of the maximum compression being perpendicular to the belt axis (Pierdominici and Heidbach, 2012; Montone and Mariucci, 2016; Figs. 1 and 4). In the northern sector (offshore Marche region, Fig. 3) focal mechanism solutions of earthquakes depict a transpressive stress regime (Pondrelli *et al.*, 2011). Seismic data from the 2013 Marche

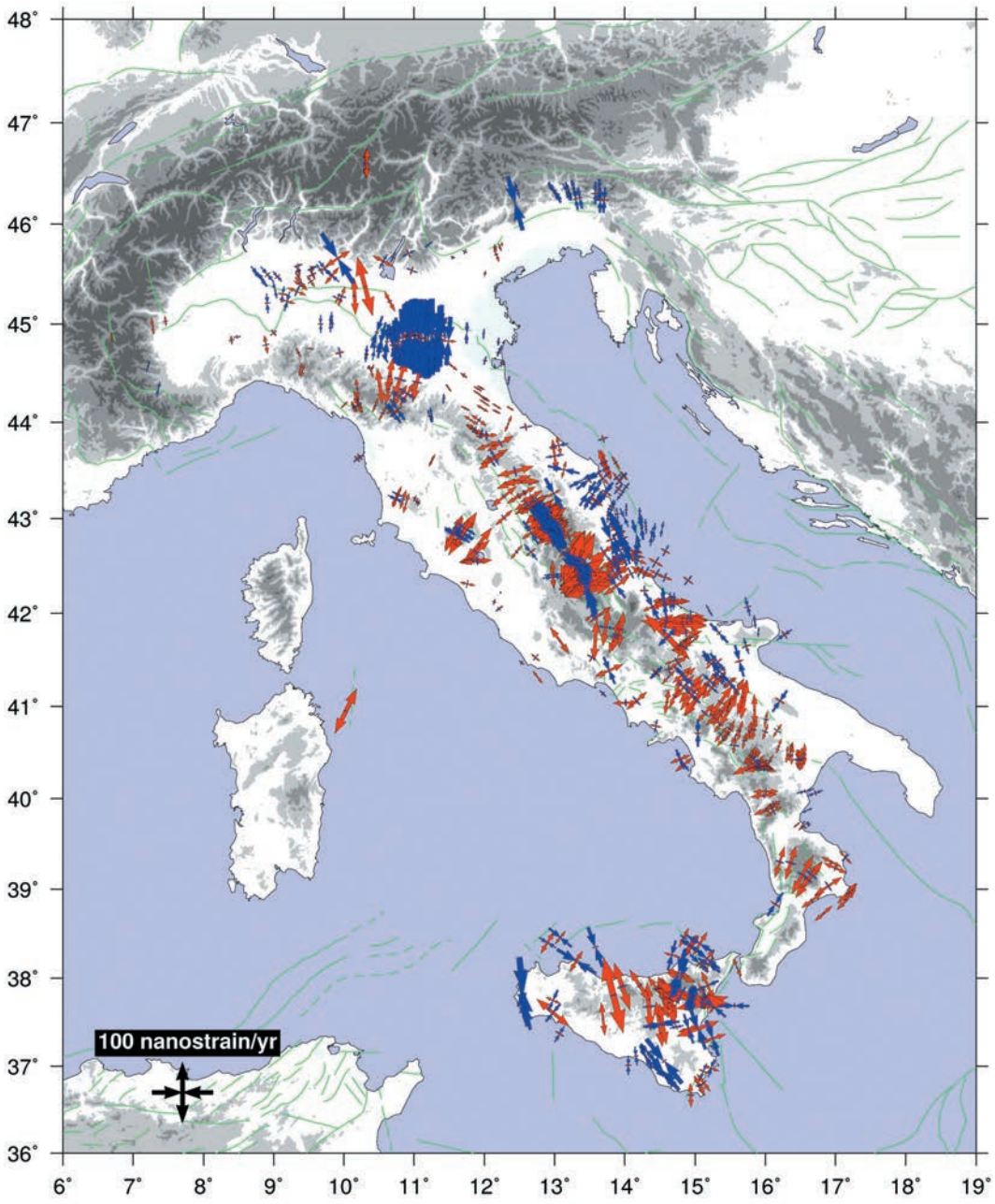

Fig. 4 - Eigenvectors of the strain-rate tensor inferred from GPS velocities interpolated at the position of those wells and focal mechanisms in the stress map sufficiently covered by GPS data. Extension is shown in red and compression in blue. Green lines show major faults.

seismic sequence, analyzed by Mazzoli *et al*. (2015), confirmed that seismicity in this area is more likely related to crustal strike-slip faulting.

Further to the south, the extension-compression pair is still observed across the Calabrian Arc. Here, the tectonic pattern along the Ionian coast is not well identified by geodetic and seismic data (e.g., Serpelloni *et al*., 2007; D'Agostino *et al*., 2008) while along the Tyrrhenian

side focal solutions and historical normal-faulting earthquakes clearly depict an on land extensional tectonics (e.g., Tortorici *et al.,* 1995; Chiarabba *et al.,* 2005; Neri *et al.,* 2006; Pondrelli *et al.,* 2011). Principal directions of extension follow the curvature of the Calabrian Arc, then progressively varying from almost ENE-WSW at the northern tip to NW-SE across the Messina Straits. Extension propagates southwards, perpendicular to the northern Sicilian Maghrebides belt extending along the Tyrrhenian coast of Sicily. Focal solutions of shallow earthquakes offshore northern Sicily are highly consistent, and outline a narrow compressive belt (Billi *et al.,* 2011; Pondrelli *et al.,* 2011; Montone and Mariucci, 2016), with P-axes ~N-S oriented. East of Aeolian Islands, extensional to strike-slip mechanisms occur along a nearly NNW-SSE alignment, which connects the archipelago to Mount Etna, and continues toward the south along the eastern Sicily escarpment (Billi *et al.,* 2007).

The roughly N-S convergence between African and Eurasian plates is the first-order mechanism that leads the kinematics of the Adria Plate or the ensemble of independent microblocks of which it is composed [according to Calais *et al*. (2002), D'Agostino *et al*. (2008), and Sani *et al*. (2016)]. The push of the Adriatic lithosphere against the southern and eastern Alps results into a broad compressional indentation that extends between Giudicarian Alps to the west and Dinarides to the east. In this area, geodetic, structural, seismic and geophysical data agree in depicting a prevailing compressive kinematics with mainly ~N-S direction of compression (e.g., Caporali and Martin, 2000; Montone adnd Mariucci, 2016; Sani *et al.,* 2016; Serpelloni *et al.,* 2016) which are in part interleaved with strike-slip faults (Montone and Mariucci, 2016; Sani *et al.,* 2016).

3. Input data

3.1. Italian contemporary stress map

Montone and Mariucci (2016) released an updated stress map that includes data from different stress indicators such as borehole breakouts, earthquake focal mechanisms, active faults and formal inversion of seismic sequences (Fig. 1). The new stress map shows minimum horizontal stress orientation (Sh_{min}) for 630 points, with a good coverage of the most seismically active areas in the Italian territory. The stress orientations included in the map of Montone and Mariucci (2016) have quality A to C and a maximum associated uncertainty of 25°. D-quality data have an uncertainty between 25° and 40°. Based on the World Stress Map guidelines (Heidbach *et al.,* 2010) all single focal mechanisms have to be considered C quality (stress orientation uncertainty in the range of ±25°).

We focus our analysis on stress data from borehole breakouts (A to D quality) and earthquake focal solutions. The latter is the most abundant set of data in the Italian Stress Map (~60%), and together with borehole measurements represents over 90% of the whole stress data set. The two techniques sample almost the whole thickness of the brittle seismogenic crust with borehole breakouts providing information about the state of stress in the first kilometres (typically up to ~5 km) while focal solutions are the only stress indicator available at higher depth [mostly up to 20 km and sometimes reaching depths of 40 km (Zoback and Zoback, 1989; Heidbach *et al.,* 2010; Montone and Mariucci, 2016)]. Directions of the principal stresses from focal mechanisms of events with $M_w \geq 4$ are estimated as the average orientation for compression,

null and extension axes (Zoback and Zoback, 1989; Heidbach *et al.*, 2010). Borehole breakouts represent a shear failure of the borehole wall along Sh_{min}, the azimuth of the minimum horizontal stress. For each well, the instantaneous state of stress in its vicinity is statistically estimated as the weighted mean direction of a population of breakouts measured along the borehole (Zoback, 1992; Ljunggren *et al.,* 2003). They are a valuable stress indicator especially in aseismic regions, where stress data from focal mechanisms and faults are not available.

3.2. GPS data and velocity field

INGV, some universities and local administrations developed a network that currently includes over 600 permanent GPS sites distributed all along the Italian territory, which are routinely processed according to internationally agreed standards (http://epncb.oma.be/_documentation/guidelines/guidelines_analysis_centres.pdf) to generate velocities in the latest realization of the ITRF frame (IGb08 at this time). The database of position and velocities maintained at the University of Padova (http://retegnssveneto.cisas.unipd.it) is updated regularly and provides logsheets, weekly solutions, cumulative solutions (from weekly normal equations stacking), time series and a "discontinuity file" with the solution numbers introduced to account for discontinuities in the time series of each processed site. Velocities of over 500 sites with at least two years of continuous tracking and accurately verified time series are published.

Fig. 2 shows the horizontal GPS velocities with respect to Eurasia (ETRF2000) for the Italian peninsula and surrounding regions. The better distribution and the increased number of GPS stations allow to identify the main kinematic features characterizing the study area. Velocities clearly depict the Apennines axis as a boundary between two kinematic domains, with NE-ward and NNW-ward oriented vectors along the Adriatic and Tyrrhenian side, respectively. The Corsica-Sardinia block and north-western Italy behave as rigid blocks with almost null residuals in an Eurasia-fixed frame. On the NE (Veneto and Friuli regions), GPS velocities show a counterclockwise rotation related with the motion of Adria Plate with respect to Eurasia. NNW-ward velocity vectors increase in magnitude moving toward east from Emilia region to Friuli, while a rapid decrease is observed moving toward the Alps. In the southernmost sectors of the study area, Sicily and the Calabrian Arc show a strongly variable velocity field where the Messina Strait acts as a structural discontinuity. Moving toward east, vectors rotate from NW-ward direction in the Sicilian domain to NE-ward direction along the Calabria region. A complex pattern of velocity gradients is also observed within Sicily island linked to its internal fragmentation.

4. From GPS velocities to strainrate: methodologies

Various approaches have been proposed to study the crustal deformation at regional or globalscale, most of them use discrete observation on the Earth surface to estimate continuous strain-rate fields (Kreemer *et al.,* 2014). A complete analysis of the various computation algorithms is beyond the scope of this work, and we present here just a brief overview. The classic procedure to estimate geodetic strain is based on triangulation of the study area (e.g., using Delauney method) and estimation of deformation within each triangle. Shen *et al.* (1996) used this approach to estimate an interpolated velocity field that takes into account

the distribution of GPS stations and velocities uncertainties. In their approach strain and rotation rates are estimated from the velocity data through weighted least squares where the contribution of each station is weighted inversely to its distance. However, the discretization of the investigated area into triangles implies a lack of redundancy of data and outliers are difficult to detect. Pietrantonio and Riguzzi (2004) implemented an algorithm to estimate geodetic strain-rate fields following an estimation strategy where the starting hypothesis of homogeneity is tested and a subdivision into sub-domains is allowed once the condition of data redundancy is verified. To account for the different length scales that characterize deformation phenomena at the Earth surface, Tape *et al*. (2009) proposed a multiscale approach based on the linear combination of spherical wavelets to describe the velocity field on the Earth surface. According to this approach, velocities at given points are computed as a superposition of values estimated at different spatial scales. Unlike studies based on physical model parametrization, where an a-priori description of the system is required [e.g., block bounding faults geometry into the block modeling of Meade and Loveless (2009)], this non-physical procedure allows to detect signals from unknown sources. In 1993, Haines and Holt (1993) developed a method to calculate continuous velocity gradient tensor field at the plate boundary zones using bi-cubic spline function to interpolate sparse geodetic data. The Haines and Holt (1993) method, adopted by many subsequent studies of crustal deformation (e.g., Hackl *et al*., 2009; Kreemer *et al*., 2014) includes also strain-rate observations from seismological and geological data. Caporali *et al*. (2003) analyzed the relation between crustal stress and strain estimating the geodetic strain-rate field from a dense network of GPS stations. He proposed an approach based on a least-square collocation algorithm where the scattered GPS velocities are interpolated at the interest points, and their contribution is weighted by a covariance function inversely proportional to their squared distance and scaled by the velocity data themselves. The velocity gradient is then estimated trough horizontal differentiation of the interpolated velocities. For a given data set, different approaches might yield to different estimations of strain. Each developed computation algorithm has its own strengths and weaknesses and shows different levels of sensitivity to different parameters, such as data sparseness or error budget. Wu *et al*. (2011) carried out an analysis of several methods to compute GPS strain-rate fields. They defined and compared two groups of strain computation methods, segment and gridded methods, and run various simulations to test their robustness, reliability and stability. The authors concluded that least-square collocation method yields to best results in terms of robustness, edge effect, error distribution and stability recognizing as the most important strength of this approach the capability of reproducing the real distribution of GPS velocities.

In this work we apply the approach described in Caporali *et al*. (2003) which uses the collocation algorithm to estimate a continuous 2D strain-rate field starting from a data set of more than 500 GPS velocities scattered on the Italian peninsula and surroundings. To compare geophysical and GPS inferred stress directions we need to estimate geodetic strainrates at the same locations (P_i) as boreholes and focal mechanisms. For this purpose, it is necessary that a sufficiently large number of GPS stations are available to compute a horizontal gradient in the neighborhood of each P_i point within a correlation distance d_0 of the order of some tens of kilometres. The concept of correlation distance for the computation of a strain rate is conveniently embodied into the algorithm of least squares collocation. Least squares collocation is an autoregressive algorithm, where the velocity interpolated at a point P is expressed as a

weighted average of the velocities measured at points i (i=1..n), with weight function decreasing with the distance from P to the i-th GPS site. To decrease the weight of spurious data, perhaps affected by local disturbances, we apply a low pass filter that results in smoothing the estimated velocity field. The horizontal gradient of the computed velocities at P_i follows from their differentiation in the north and east directions. The 2D strain rate is the symmetrical part of the velocity gradient. The eigenvalues and eigenvectors of the strain-rate tensor are computed by matrix diagonalization, yielding a maximum/minimum strain rate (typically the most extensional/compressional, corresponding to a positive/negative horizontal derivative of the velocity field), and the azimuth ϑ of the most extensional strain rate. Hence ϑ corresponds to Sh_{min}. We compute one correlation distance d_0 for each point P_i, by analyzing the correlation profile of the local GPS site velocities. For each point we compute the shear strain rate at increasing values of the correlation distance, to find the value of d_0 which maximizes the shear strain rate. This ensures that all the correlated velocities contribute to the computation of the strain-rate tensor.

5. Results

5.1. Geodetic strain-rate field

We use the least-squares collocation algorithm described above to interpolate velocities from over 500 GPS stations and estimate the strain-rate eigenvectors at the locations of wells and focal solutions in the Italian stress map (Fig. 4). Only stress data surrounded by a reliable number of GPS stations (minimum 4 within the correlation distance) are used as interpolation points (Figs. 1 and 2). Although a significant number of boreholes is found offshore (Fig. 1), their proximity to the coast often provides a sufficient coverage of GPS data and only 21 wells are discarded from strain-rate computations. We were able to estimate strain-rate eigenvectors for 317 focal mechanisms data over a total number of 392. Most of the rejected focal solutions are distributed around Tyrrhenian basin, Adriatic and Ionian seas, areas with a total absence of GPS observations. In the end, each strain-rate value is computed with the contribution of an average number of 10 GPS stations lying within an average correlation distance of 62 km. For both, wells and earthquake data, we find correlation distances between 50 and 140 km with populations of GPS sites ranging from 4 to 27. About 90% of the strainrates are computed by comparing velocities of at least 14 GPS stations within the correlation distance.

The uncertainties associated with the strain-rate values are estimated on the base of the uncertainties of the GPS velocities. Assuming a minimum number of 4 GPS stations, an average radius of about 60 km, a conservative uncertainty of 0.2 mm/yr for the GPS velocities and their statistical independence, we find an uncertainty of ~8 nstrain/yr to be associated with each strain-rate estimation. Then, being ~40 nstrain/yr the average value of strainrate in our investigated area, we infer about 10° as mean uncertainty on the azimuth angle of the geodetic principal stress. Fig. 4 shows the computed eigenvectors of the strain-rate tensor. Owing to the uneven spatial distribution of the geophysical stress data, most of the arrows displaying the maximum extensive and compressive strainrates are concentrated in a few areas resulting in an irregular and unclear graphical interpretation of the strain-rate field. However, the main deformation patterns are identifiable across the principal active tectonic regions on the Italian peninsula. In agreement with the available seismic, geological and geophysical data, we find

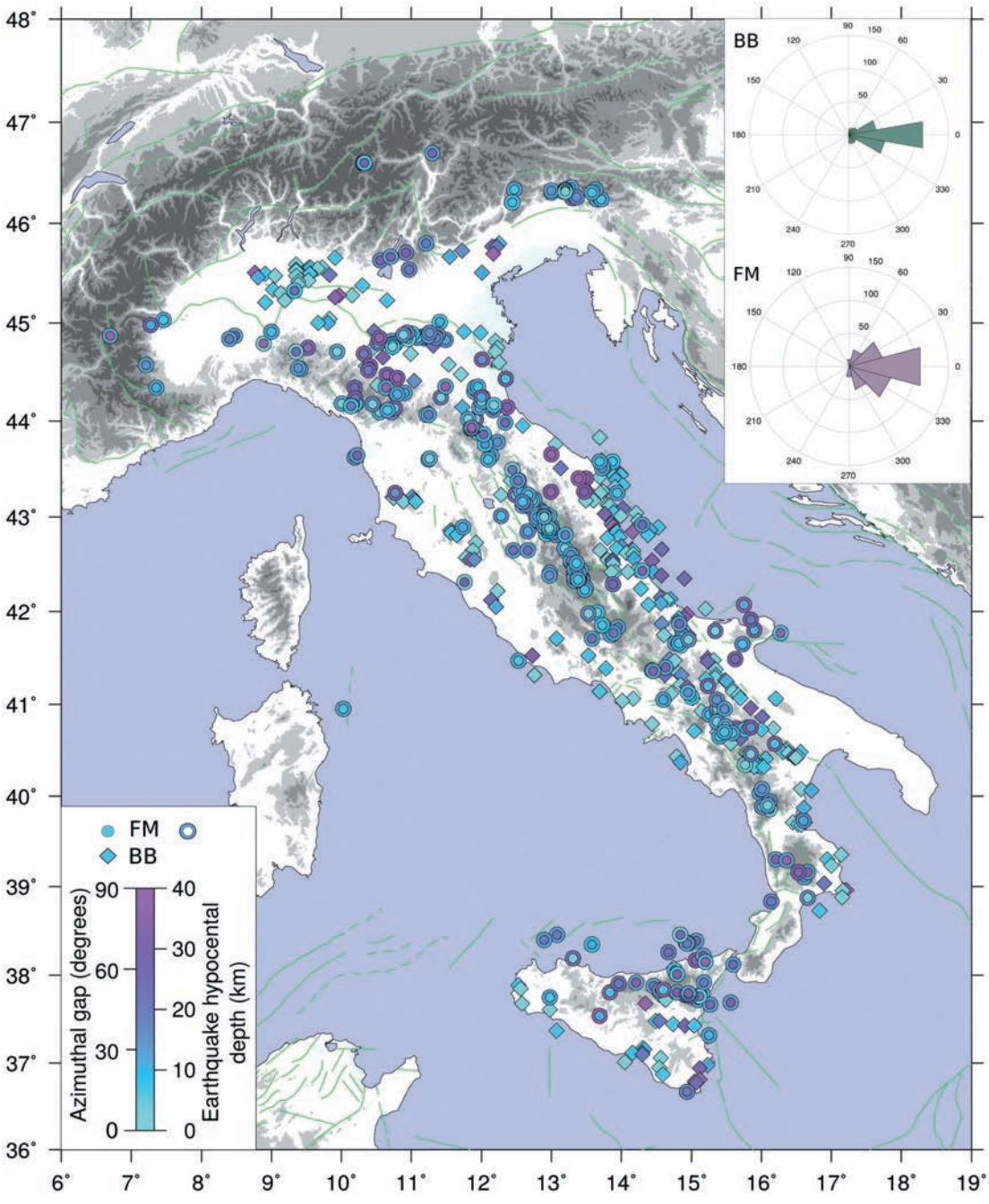

Fig. 5 - Difference (in absolute value) in azimuth of minimum horizontal stresses between each borehole or focal mechanism measurement, and the geodetically inferred strain-rate direction of extension. Diamond symbols refer to stress data from borehole breakouts (BBs), circles to focal mechanisms (FMs); rings represent the hypocentral depth of each earthquake. Color homogeneity of circles and their own rings indicates correlation between magnitude of azimuthal discrepancies and hypocentral depth of the earthquake. Insert on the top-right corner shows the angular distribution of the azimuthal differences between stress orientation from BBs or FMs and geodetic strain-rate direction. The rose histograms show the weighted azimuthal differences between each stress and strain-rate direction. The width of the bins is defined on the base of the stress data uncertainties: for BBs data we estimate a square root of the average quadratic uncertainties of ~18° that is approximated to 20° as angle bin. For FM data, we approximate the 25° fixed uncertainty to a 30° bin.

that a mostly extensive deformation characterizes the whole Apennine mountains belt with the maximum extension running almost perpendicular to the belt axis. Strong compression in a roughly N-S direction is observed across the Emilia and Friuli regions and southern Tyrrhenian, though the latter is characterized by a more complex pattern with the direction of compression rotating clockwise moving eastwards along the northern coast of Sicily. In agreement with what argued by Mazzoli *et al*. (2015), geodetic data highlight an undefined deformation pattern for the outer Apennines region where a mix of compressive and extensive strainrate of variable orientations are observed within one hundred kilometres.

5.2. Comparison between geodetic strain and geophysical stress orientations

We focus on the difference in azimuth of minimum horizontal stresses (geodetic Sh_{min} - geophysical Sh_{min}) between each focal mechanism or borehole measurement, and the geodetically inferred direction. We consider separately the two data sets because they are different stress indicators with a different degree of reliability. All the focal mechanisms data are ranked C quality (25° of uncertainty), whereas wells data have uncertainties varying from 0 to 40°. To account for the different quality levels of the stress orientations of breakouts, we calculate the angular discrepancy with the geodetic Sh_{min} as the weighted difference, with weights inversely proportional to the uncertainties on the geophysical data. Overall, we observe a slightly better agreement between geodetic and boreholes stress orientations with a weighted mean discrepancy of -17° and a wrms (weighted root mean square) uncertainty of 33°. The mean angular difference between GPS and focal mechanisms Sh_{min} is -4° and the rms (root mean square) uncertainty is 40° (insert in Fig. 5).

The selection criterion used by the least-squares collocation approach guarantees the contribution of a minimum number of GPS data in the computation, but does not account for their homogeneous spatial distribution. We focus our analysis on stress data in regions with a dense coverage of GPS sites, and subdivide them according to the stress regime. We define five provinces (polygons in Fig. 1): two of them, central and southern Apennines, are subject to extension roughly perpendicular to the belt, Emilia and Friuli regions show a mainly compressive tectonics, while the outer Apennines region is characterized by compressive-transpressive stress. In Table 1 we give the number of boreholes or focal mechanisms stress data falling within each of the five analyzed regions, the mean difference between geophysical

Table 1 - Analysis of angle gap between minimum horizontal stress orientations from borehole (A-D quality) or focal mechanisms measurements (Montone and Mariucci, 2016) and geodetically inferred stress directions. For each investigated tectonic area we give: number of stress data, mean and root mean square of the difference between geodetic and geophysical Sh_{min}. For the boreholes data, characterized by variable uncertainties, we indicate the weighted values of mean and rms. Weights are inversely proportional to the uncertainties associated with the boreholes stress orientations.

	BOREHOLE BREAKOUTS			FOCAL MECHANISMS		
TECTONIC REGION	#	Wmean (deg)	WRMS (deg)	#	mean (deg)	RMS (deg)
Friuli	0	-	-	16	9.0	18.5
Emilia	19	17.3	29.7	20	0.4	29.8
C. Apennines	4	-	-	97	-1.3	23.0
S. Apennines	54	5.8	31.7	28	4.8	25.2
O. Apennines	40	-19.3	30.1	13	-34.5	54.3

and geodetic Sh_{min} and the associated rms. Data from wells measurements are provided with the weighted values. Weights were computed on the basis of the uncertainties of the geophysical data. Results are graphically shown in Fig. 6. For each region we plot a map with the geodetic strainrate and geophysical minimum horizontal stress orientations and a rose diagram with the distribution of the angle between them. For boreholes data the histogram shows the weighted differences and the width of each bin is defined on the base of the stress data uncertainties. We approximate the 25° of fixed uncertainty on focal mechanisms stress orientation to a 30° bin. For boreholes data we estimate a square root of the average quadratic uncertainties of ~18° that is approximated to 20° as angle bin.

5.2.1. Central Apennines

Central Apennines (Fig. 6a) are covered by a dense population of GPS sites and an elongated array of 97 stress data from focal mechanisms along the belt axis. Both the estimated geodetic strainrates and the stress data well depict the SW-NE orientation of the most extensional stress in this tectonic region. For more than 60% of stress data we find azimuthal discrepancies smaller than the associated mean square uncertainty with a symmetrical distribution around zero and a rms value of 23°.

5.2.2. Southern Apennines

Same observations can be done for the southern Appenines (Fig. 6b). In this sector of the belt, the stress field rests on 54 Sh_{min} measurements in wells and 28 data from seismic events. Again we find a symmetric distribution of the angular gap around the null value with a weighted mean discrepancy of ~6° and ~5° for boreholes and focal mechanisms data, respectively. Residuals are characterized by a slightly bigger dispersion with wrms values of ~32° and ~25°.

5.2.3. Outer Apennines

We defined a third tectonic province including part of the outer compressive-transpressive sector of the Appenines, between the belt axis and the Adriatic Sea. We draw the boundaries of our area based on the GPS sites distribution: we discard the offshore stress data for which the availability of the minimum number of GPS stations required by the strain-rate estimation is verified, but are still characterized by an unilateral spatial distribution of the geodetic data. This region is drilled by 40 deep wells that measure a mainly compressive stress field in SW-NE direction. The estimated Sh_{min} discrepancies are smaller than 20° for around 65% of the analyzed regional data set. We find an almost perfectly symmetrical distribution around zero with associated weighted rms of ~30°. The stress map in this area counts also 13 data from focal mechanisms that are interpreted as thrust or strike-slip events. For most of them we find an angular difference with the geodetic inferred stress orientation larger than 40°. The biggest azimuthal discrepancies, of 80°, 85° and 86°, are found for three stress data from focal solutions of deep events (labeled as 1, 2 and 3 in Fig. 6c) lying in the north-western sector of the study area. All of them refer to earthquakes with hypocentral depth between 30 and 40 km and are interpreted as strike slip events with a roughly WSW-ENE orientation of Sh_{min}. Along the same direction, GPS velocities are characterized by a compressive gradient (Fig. 4) resulting in an almost perpendicular minimum horizontal stress orientation.

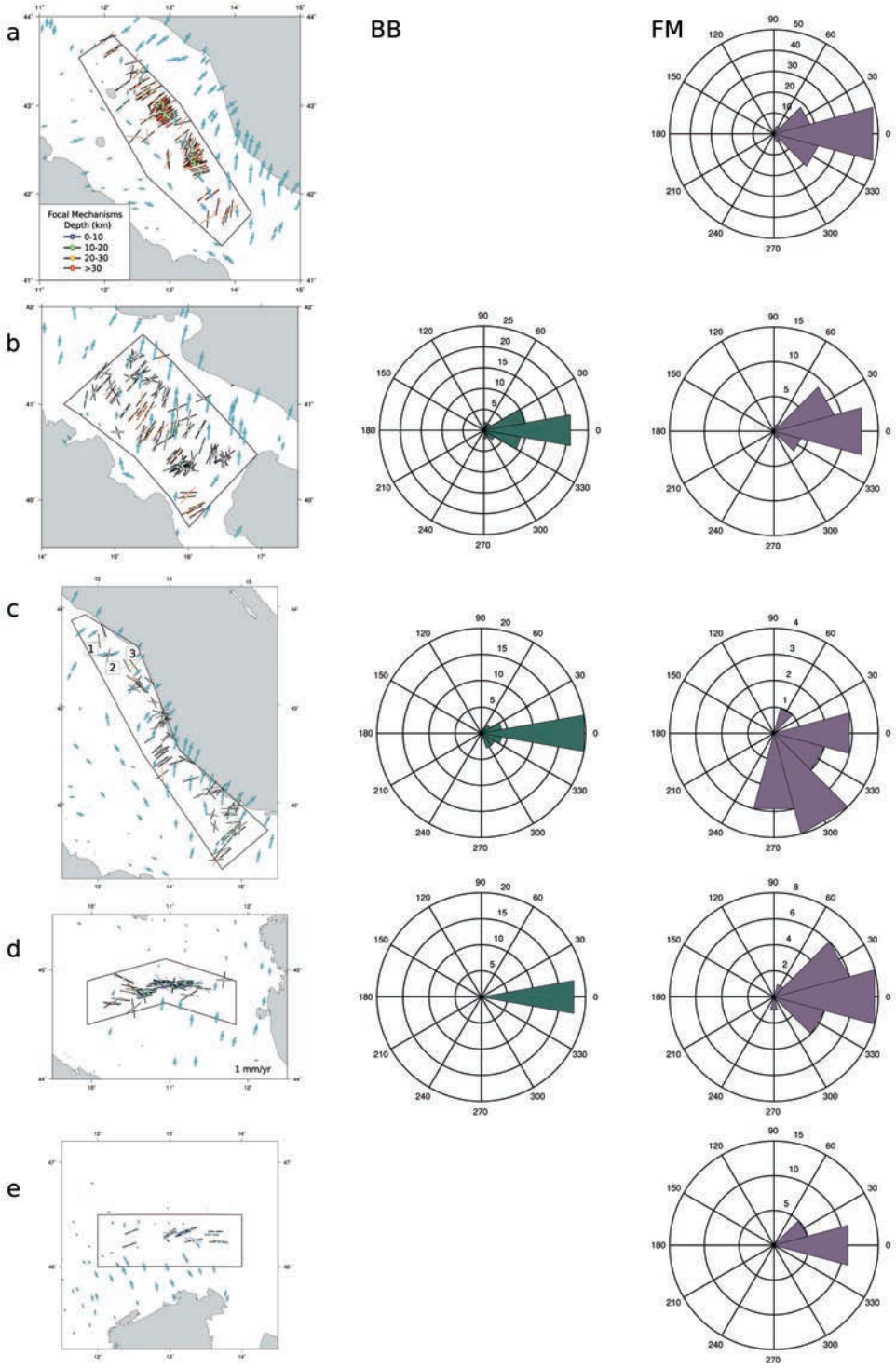

Fig. 6 - Results of our statistical analysis of the azimuthal gap between focal mechanisms and/or boreholes and geodetic Sh_{min} for the five analyzed regions (lines a to e). Left column: at each stress point, geodetic strainrate (black) and stress (symbology as in Fig. 1) orientations are shown. Depth of the focal mechanisms is represented as a color scale of the small circles. Arrows show the smoothed GPS velocity field used to estimate the geodetic strain-rate field. Central and rights columns: rose diagram with the angular distribution of the difference between geodetic and boreholes (BB) or focal mechanisms (FM) Sh_{min}. See Fig. 5 for details.

5.2.4. Emilia and Friuli

The northernmost analyzed tectonic regions, Emilia and Friuli (Figs. 6d and 6e), are small areas densely populated by GPS sites but covered by a relatively small number of stress data. Stress orientations from focal solutions and borehole breakouts show homogeneous patterns that well describe the roughly N-S compression in the two areas. The regional compressive tectonics is well imaged also by the GPS velocities and the inferred strain-rate eigenvectors. We find a good agreement between the two data sets, with mean discrepancies between focal solution and geodetic strain-rate directions of 0.4° and 9° for Emilia and Friuli, respectively. The weighted mean difference between geodetic and borehole breakouts Sh_{min} for the Emilia region is 17°. The associated rms values are consistent with the uncertainties of the geophysical data.

6. Discussion and conclusions

We used horizontal velocities from more than 500 GPS stations to estimate a strain-rate field for the Italian territory and compare it with the present-day Italian stress map. We selected data from boreholes breakout and focal mechanisms which represent over 90% of the whole stress database. In correspondence of each stress data surrounded by a sufficient number of geodetic observations, we applied a least-squares collocation algorithm to interpolate the GPS velocities and estimate the strain-rate eigenvectors. Assuming an elastic rheology for the upper crust enables us to consider the orientation of the stress and strain-rate eigenvectors as roughly parallel. We calculated the angle gap between minimum horizontal stresses from boreholes or focal mechanism SDC measurements and the geodetically inferred strain-rate direction of extension.

Our analysis highlighted that Sh_{min} orientations form stress indicators and geodetic data are roughly parallel for most of the investigated area. For more than 50% of the stress data from focal mechanisms we find azimuthal discrepancies smaller than the associated uncertainty of 25°. Comparison of boreholes and GPS Sh_{min} orientations shows that about 60% of the angular differences are within one standard deviation. The residuals have a nearly symmetric spread about zero with weighted rms of 33° and 40° for boreholes and focal mechanisms data, respectively. The corresponding weighted averages are about -3° and -16°. Hence, we conclude that the geophysical and geodetic stress orientations agree within one standard deviation.

Fig. 5 shows that geodetic surface deformation and crustal stress from seismic and well data almost overlap, in terms of Sh_{min} orientation, along the whole central and southern Apennine belt. Both the strain-rate and stress fields show as main tectonic feature a uniform SW-NE extension almost perpendicular to the belt axis. Such an agreement results in an elongated NW-SE oriented strip of points that are, for the most part, characterized by azimuthal gaps lower than 30°. Seismicity in this area is mostly concentrated within the first kilometres depth, about 80% of the focal solutions in the local stress map refers to earthquakes with hypocentral depth lower than 10 km and nearly all, but just a few sparse events, lie within the first 20 km, in the elastic layer of the crust. In the southern sector of the belt, stress data from seismic indicators are flanked by an array of wells distributed parallel to the belt axis. Sh_{min} orientations inferred from boreholes breakouts are in agreement with data from focal mechanisms.

In Friuli and Emilia regions Sh_{min} values are centred around 90°. This indicates a main E-W direction of extension in agreement with the other available seismological, geological and

geodetic data discussed above, that describe the two study regions as compressional domains where compression is ~N-S oriented. Our results show that the orientations of minimum horizontal stress inferred from seismic and borehole measurements and the geodetic strain-rate directions of extension agree within one standard deviation for both the investigated areas.

Fig. 5 shows that all the analyzed points with angular residuals larger than 80°, then approximately perpendicular intersection of stress and strain-rate fields, are placed along a narrow bend that extends to the east of the northern-central Apennines, following the NW-ward curvature of the belt axis from the Adriatic coast of Marche region up to the Po Plain area. An abrupt change of the tectonic regime characterizes this transition zone lying between the Apennine extensional domain and the mostly compressional outer Apennines. In the coastal sector a reliable estimation of the surface deformation field is supported by a fairly dense network of GPS stations, whereas in the inner zone, between the northern Apennine arc and the Po Valley, it rests on a few scattered data. This region is sampled by a large number of stress data from focal mechanisms, many of whose, from deep events. Interestingly, most of the stress data in this area affected by discrepancies larger than 80° are estimated from earthquakes deeper than 20 km.

We investigated the correlation between hypocentral depth and azimuthal differences of Sh_{min} directions for all the stress data from focal mechanisms in our data set. Most of the focal mechanisms data in the Italian stress map come from shallow events with hypocentres within the first 20 km. However 15% of them refers to deep earthquakes within 20 and 40 km. Analyzing the mean stress orientation at different depths for the Italian territory, Pierdominici and Heidbach (2012) found no significant differences between shallow and deep neighboring stress indicators. However, comparing co-located stress and strain-rate directions for the data deeper and shallower than 20 km we find that they seem characterized by different behaviors. Histograms in Fig. 7 show that azimuthal residuals of shallow data are normally distributed around zero, whereas for the deeper data we find an almost random relationship between number of points and their associated angular discrepancies. As discussed, comparing stress and strain-rate eigenvectors implies comparing data sampled at the Earth surface (the geodetic velocity gradient) with data from the whole thickness of the upper crust (the geophysical stress data). The assumption that they are parallel down to ~20 km depth rests on a model of the brittle

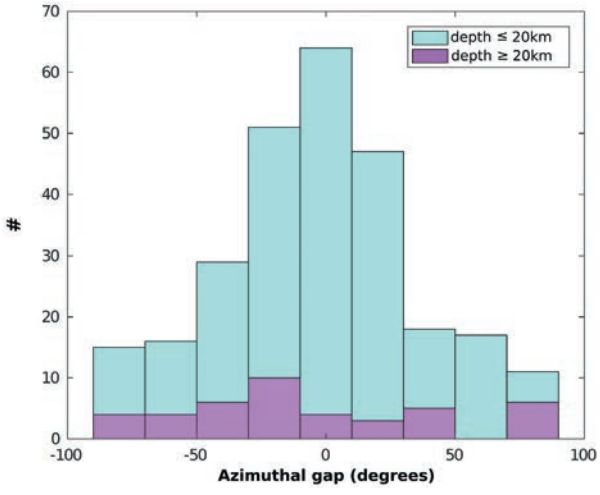

Fig. 7 - Distribution of the focal mechanism data as a function of the azimuthal discrepancies between Sh_{min} and geodetic strain-rate directions. Bins colored in cyan and magenta refer to shallow (depth ≤ 20 km) and deep (depth ≥ 20 km) earthquakes, respectively.

upper crust characterized by elastic rheology. When we take into account deep measurements we also assume that crustal stress at depth and surface deformation are generated by the same process as well as its depth independence. The tectonics of northern and outer Apennines region is driven by the subduction of the Adria Plate beneath the Apennines that generates the deep seismicity distributed along this segment of the Adriatic coast and following, on-land, the Apennines belt (Salimbeni *et al.,* 2013; Mazzoli *et al.,* 2015). Hence, we cannot exclude that the ground deformation observed by the GPS stations in this area is decoupled from the mechanisms that generate seismicity at depth. In fault plane solutions the zones of compression and dilatation vary with depth and this could be a reason for the stress at depth be different from the deformation measured at the surface. However, several other explanations may be proposed. More generally, local stress rotations not recorded by surface strain-rate data could explain the observed discrepancies. This is the case, for example, when stress is transferred from an earthquake to a nearby receiver fault in a regime of low regional stress.

Knowing the present-day state of crustal stress and deformation is a key point in terms of seismic hazard. The fast development, in the last decades, of geophysical and geodetic techniques has resulted in a significant increase in the availability of information and a better quality and spatial coverage of data. This gives us the opportunity of comparing independent measurements of such quantities investigating the tectonic processes at the different depths in the Earth crust. Analyzing the stress and strain-rate fields for the Italian territory we find an overall reasonable agreement between stress orientations included in the Italian stress map and based on focal mechanisms or borehole measurements and the estimated strain-rate field computed on the base of the horizontal GPS velocities for the whole study area.

Acknowledgements. The authors gratefully acknowledge the constructive review of two anonymous reviewers and the suggestions of the editor. Brunella Mastrolembo gratefully acknowledges the grant of the University of Padova at the Department of Geosciences, where the research was carried out.

REFERENCES

Barba S., Carafa M.M.C. and Boschi E.; 2008: *Experimental evidence for mantle drag in the Mediterranean*. Geophys. Res. Lett., **35**, L06302, doi:10.1029/2008GL033281.

Billi A., Gambini R., Nicolai C. and Storti F.; 2007: *Neogene - Quaternary intraforeland transpression along a Mesozoic platform-basin margin: the Gargano Fault system, Adria, Italy.* Geosphere, **3**, 1-15.

Billi A., Faccenna C., Bellier O., Minelli L., Neri G., Piromallo C., Presti D., Scrocca D. and Serpelloni E.; 2011: *Recent tectonic reorganization of the Nubia - Eurasia convergent boundary heading for the closure of the western Mediterranean.* Bull. Soc. Geol. Fr., **182**, 279-303.

Bruyninx C., Altamimi Z., Caporali A., Kenyeres A., Stangl G. and Torres J.A.; 2013: *Guidelines for EUREF densifications*, *vers. 5*, <epncb.oma.be/pub/general/Guidelines_for_EUREF_Densifications.pdf>

Calais E., Nocquet J., Jouanne F. and Tardy M.; 2002: *Current strain regime in the western Alps from continuous Global Positioning System measurements, 1996-2001*. Geol., **3**, 651-654, doi:10.1130/0091-7613a.

Caporali A. and Martin S.; 2000: *First results from GPS measurements on present day alpine kinematics*. J. Geodyn., **30**, 275-283.

Caporali A., Martin S. and Massironi M.; 2003: *Average strain rate in the Italian crust inferred from a permanent GPS network-II. Strain rate versus seismicity and structural geology.* Geophys. J. Int., **155**, 254-268.

Caporali A., Neubauer F., Ostini L., Stangl G. and Zuliani D.; 2013: *Modeling surface GPS velocities in the southern and eastern Alps by finite dislocations at crustal depths*. Tectonophys., **590**, 136-150, doi:10.1016/j.tecto.2013.01.016.

Carafa M.M.C. and Barba S.; 2013: *The stress field in Europe: optimal orientations with confidence limits*. Geophys. J. Int., **193**, 531-548, doi:10.1093/gji/ggt024.

Carafa M.M.C. and Bird P.; 2016: *Improving deformation models by discounting transient signals in geodetic data, II: geodetic data, stress directions, and long-term strain rates in Italy.* J. Geophys. Res., **121**, 5557-5575, doi:10.1002/2016JB013038.

Carafa M.M.C., Barba S. and Bird P.; 2015: *Neotectonics and long-term seismicity in Europe and the Mediterranean region*. J. Geophys. Res., **120**, 5311-5342, doi:10.1002/2014JB011751.

Chiarabba C., Jovane L. and Di Stefano R.; 2005: *A new view of Italian seismicity using 20 years of instrumental recordings*. Tectonophys., **395**, 251-268, doi:10.1016/j.tecto.2004.09.013.

D'Agostino N., Avallone A., Cheloni D., D'Anastasio E., Mantenuto S. and Selvaggi G.; 2008: *Active tectonics of the Adriatic region from GPS and earthquake slip vectors*. J. Geophys. Res., **113**, B12413, doi:10.1029/2008JB005860.

D'Agostino N., England P., Hunstad I. and Selvaggi G.; 2014: *Gravitational potential energy and active deformation in the Apennines*. Earth Planet. Sci. Lett., **397**, 121-132.

DeMets C., Gordon R.G. and Argus D.F.; 2010: *Geologically current plate motions*. Geophys. J. Int., **181**, 1-80, doi:10.1111/j.1365-246X.2009.04491.x.

Di Bucci D., Ridente D., Fracassi U., Trincardi F. and Valensise G.; 2009: *Marine palaeoseismology from very high resolution seismic imaging: the Gondola Fault zone (Adriatic foreland)*. Terra Nova, **21**, 393-400, doi:10.1111/j.1365-3121.2009.00895.x.

DISS Working Group; 2015: *Database of Individual Seismogenic Sources (DISS), Version 3.2.0: a compilation of potential sources for earthquakes larger than M 5.5 in Italy and surrounding areas*. Istituto Nazionale di Geofisica e Vulcanologia, Roma, Italy, doi:10.6092/INGV.IT-DISS3.2.0, <diss.rm.ingv.it/diss/.>.

Faccenna C., Becker T.W., Lucente F., Jolivet L. and Rossetti F.; 2001: *History of subduction and back-arc extension in the central Mediterranean*. Geophys. J. Int., **145**, 809-820, doi:10.1046/j.0956-540x.2001.01435.x.

Faccenna C., Becker T.W., Auer L., Billi A., Boschi L., Brun J., Pitanio F.A., Funiciello F., Horvàth F., Jolivet L., Piromallo C., Leigh Royden L., Rossetti F. and Serpelloni E.; 2014: *Mantle dynamics in the Mediterranean*. Rev. Geophys., **52**, 283-332, doi:10.1002/2013RG000444.

Hackl M., Malservisi R. and Wdowinski S.; 2009: *Strain rate patterns from dense GPS networks*. Nat. Hazards Earth Syst. Sci., **9**, 1177-1187, doi:10.5194/nhess-9-1177-2009.

Haines A.J. and Holt W.E.; 1993: *A procedure for obtaining the complete horizontal motions within zones of distributed deformation from the inversion of strain rate data*. J. Geophys. Res., **98**, 12057-12082.

Heidbach O., Tingay M., Barth A., Reinecker J., Kurfeß D. and Muller B.; 2008: *The World Stress Map database release 2008*. Doi:10.1594/GFZ.WSM.Rel2008.

Heidbach O., Tingay M., Barth A., Reinecker J., Kurfeß D. and Muller B.; 2010: *Global crustal stress pattern based on the World Stress Map database release 2008*. Tectonophys., **482**, 3-15.

Heidbach O., Rajabi M., Reiter K., Ziegler M. and the WSM Team; 2016: *World Stress Map database release 2016*. GFZ Data Services, Potsdam, Germany, doi:10.5880/WSM.2016.001.

Kastelic V. and Carafa M.M.C.; 2012: *Fault slip rates for the active external Dinarides thrust and fold belt*. Tectonics, **31**, TC3019, doi:10.1029/2011TC003022.

Kreemer C., Blewitt G. and Klein E.C.; 2014: *A geodetic plate motion and Global Strain Rate model*. Geochem., Geophys., Geosyst., **15**, 3849-3889, doi:10.1002/2014GC005407.

Ljunggren C., Chang Y., Janson T. and Christiansson R.; 2003: *An overview of rock stress measurement methods*. Int. J. Rock. Mech. Mi. Sci., **40**, 975-989.

Malinverno A. and Ryan W.B.F.; 1986: *Extension in the Tyrrhenian Sea and shortening in the Apennines as a result of arc migration driven by sinking of the lithosphere*. Tectonics, **5**, 227- 245.

Mastrolembo Ventura B., Serpelloni E., Argnani A., Bonforte A., Bürgmann R., Anzidei M., Baldi P. and Puglisi G.; 2014: *Fast geodetic strain-rates in eastern Sicily (southern Italy): new insights into block tectonics and seismic potential in the area of the great 1693 earthquake*. Earth Planet. Sci. Lett., **404**, 77-88.

Mazzoli S., Santini S., Macchiavelli C. and Ascione A.; 2015: *Active tectonics of the outer northern Apennines: Adriatic vs. Po Plain seismicity and stress fields*. J. Geodyn., **84**, 62-76, doi:10.1016/j.jog.2014.10.002.

Meade B.J. and Loveless J.P.; 2009: *Block modeling with connected fault-network geometries and a linear elastic coupling estimator in spherical coordinates*. Bull. Seismol. Soc. Am., **99**, 3124-3139, doi:10.1785/0120090088.

Montone P. and Mariucci M.T.; 2016: *The new release of the Italian contemporary stress map*. Geophys. J. Int., **205**, 1525-1531, doi:10.1093/gji/ggw100.

Neri G., Oliva G., Orecchio B. and Presti D.; 2006: *A possible seismic gap within a highly seismogenic belt crossing Calabria and eastern Sicily, Italy.* Bull. Seismol. Soc. Am., **96**, 1321-1331, doi:10.1785/0120050170.

Nocquet J.M.; 2012: *Present-day kinematics of the Mediterranean: a comprehensive overview of GPS results*. Tectonophys., **579**, 220-242, doi:10.1016/j.tecto.2012.03.037.

Palano M.; 2015: *On the present-day crustal stress, strain-rate fields and mantle anisotropy pattern of Italy.* Geophys. J. Int., **200**, 967-983, doi:10.1093/gji/ggu451.

Petricca P., Carafa M.M.C., Barba S. and Carminati E.; 2013: *Local, regional, and plate scale sources for the stress field in the Adriatic and Periadriatic region*. Mar. Pet. Geol., **42**, 160-181, doi:10.1016/j.marpetgeo.2012.08.005.

Pierdominici S. and Heidbach O.; 2012: *Stress field of Italy - mean stress orientation at different depths and wavelength of the stress pattern*. Tectonophys., **532**, 301-311.

Pietrantonio G. and Riguzzi F.; 2004: *Three-dimensional strain tensor estimation by GPS observations: methodological aspects and geophysical applications*. J. Geodyn., **38**, 1-18.

Pondrelli S., Salimbeni S., Ekstrm G., Morelli A., Gasperini P. and Vannucci G.; 2006: *The Italian CMT data set from 1977 to the present*. Phys. Earth Planet. Inter., **159**, 286-303, doi:10.1016/j.pepi.2006.07.008.

Pondrelli S., Salimbeni S., Morelli A., Ekström G., Postpischl G., Vannucci G. and Boschi E.; 2011: *European-Mediterranean Regional Centroid Moment Tensor catalog: solutions for 2005-2008*. Phys. Earth Planet. Inter., **185**, 74-81, doi:10.1016/j.pepi.2011.01.007.

Salimbeni S., Pondrelli S. and Margheriti L.; 2013: *Hints on the deformation penetration induced by subductions and collision processes: seismic anisotropy beneath the Adria region (central Mediterranean)*. J. Geophys. Res., **118**, 5814-5826, doi:10.1002/2013JB010253.

Sani F., Vannucci G., Boccaletti M., Bonini M., Corti G. and Serpelloni E.; 2016: *Insights into the fragmentation of the Adria Plate*. J. Geodyn., **102**, 121-138, doi:10.1016/j.jog.2016.09.004.

Serpelloni E., Anzidei M., Baldi P., Casula G. and Galvani A.; 2005: *Crustal velocity and strain-rate fields in Italy and surrounding regions: new results from the analysis of permanent and non-permanent GPS networks*. Geophys. J. Int., **161**, 861-880, doi:10.1111/j.1365-246X.2005.02618.x.

Serpelloni E., Vannucci G., Pondrelli S., Argnani A., Casula G., Anzidei M., Baldi P. and Gasperini P.; 2007: *Kinematics of the western Africa - Eurasia plate boundary from focal mechanisms and GPS data*. Geophys. J. Int., **169**, 1180-1200.

Serpelloni E., Bürgmann R., Anzidei M., Baldi P., Mastrolembo Ventura B. and Boschi E.; 2010: *Strain accumulation across the Messina Straits and kinematics of Sicily and Calabria from GPS data and dislocation modeling*. Earth Planet. Sci. Lett., **298**, 347-360, doi:10.1016/j.epsl.2010.08.005.

Serpelloni E., Vannucci G., Anderlini L. and Bennett R.A.; 2016: *Kinematics, seismotectonics and seismic potential of the eastern sector of the European Alps from GPS and seismic deformation data*. Tectonophys., **688**, 157-181, doi:10.1016/j.tecto.2016.09.026.

Sgroi T., De Nardis R. and Lavecchia G.; 2012: *Crustal structure and seismotectonics of central Sicily (southern Italy): new constraints from instrumental seismicity.* Geophys. J. Int., **189**, 1237-1252.

Shen Z.K., Jackson D. and Ge B.X.; 1996: *Crustal deformation across and beyond the Los Angeles basin from geodetic measurements*. J. Geophys. Res., **101**, 27957-27980.

Tape C., Muse P., Simons M., Dong D. and Webb F.; 2009: *Multiscale estimation of GPS velocity fields*. Geophys. J. Int., **179**, 945-971.

Tortorici L., Monaco C., Tansi C. and Cocina O.; 1995: *Recent and active tectonics in the Calabrian Arc (southern Italy)*. Tectonophys., **243**, 37-55, doi:10.1016/0040-1951(94)00190-K.

Valensise G. and Pantosti D.; 2001: *Database of potential sources for earthquakes larger than M 5.5 in Italy.* Ann. Geofis., **44**, 797-964.

Viti M., Viti E., Babbucci D., Tamburelli C., Cenni N., Baglione M. and D'Intinosante V.; 2015: *Belt-Parallel shortening in the northern Apennines and seismotectonic implications*. Int. J. Geosci., **6**, 938-961, doi:10.4236/ijg.2015.68075.

Wortel M.J.R. and Spakman W.; 2000: *Subduction and slab detachment in the Mediterranean - Carpathian region*. Sci., **290**, 1910-1917, doi:10.1126/science.290.5498.1910.

Wu Y.Q., Jiang Z.S. and Yang G.H.; 2011: *Comparison of GPS strain rate computing methods and their reliability.* Geophys. J. Int., **185**, 703-717.

Yang W. and Hauksson E.; 2013: *The tectonic crustal stress field and style of faulting along the Pacific North America Plate boundary in southern California*. Geophys. J. Int., **194**, 100-117.

Zoback M.D. and Zoback M.L.; 1989: *Stress in the Earth's lithosphere*. In: Fairbridge R.W. (ed) Encyclopedia of Earth Sciences Series, Van Nostrand Reinhold Co., New York, NY, USA, pp. 1221-1232.

Zoback M.L.; 1992: *First- and second-order patterns of stress in the lithosphere: the world stress map project*. J. Geophys. Res., **97**, 703-728.

Corresponding author: Alessandro Caporali
Dipartimento di Geoscienze, Università di Padova
Via Giovanni Gradenigo 6, 35131 Padova, Italy
Phone: +39 049 8279122; e-mail: alessandro.caporali@unipd.it